

# Rapid retrofit of substandard short RC columns with buckled longitudinal bars using CFRP jacketing

Marina L. Moretti<sup>1\*</sup>

<sup>1</sup>*School of Architecture, National Technical University of Athens, GR-106-82 Athens, Greece*

(Received November 19, 2022, Revised December 18, 2022, Accepted December 18, 2022)

**Abstract.** This experimental study investigates the effectiveness of applying carbon fiber reinforced polymer (CFRP) jackets for the retrofit of short reinforced concrete (RC) columns with inadequate transverse reinforcement and stirrup spacing to longitudinal rebar diameter equal to 12. RC columns scaled at 1/3, with round and square section, were subjected to axial compression up to failure. A damage scale is introduced for the assessment of the damage severity, which focusses on the extent of buckling of the longitudinal rebars. The damaged specimens were subsequently repaired with unidirectional CFRP jackets without any treatment of the buckled reinforcing bars and were finally re-tested to failure. Test results indicate that CFRP jackets may be effectively applied to rehabilitate RC columns (a) with inadequate transverse reinforcement constructed according to older practices so as to meet modern code requirements, and (b) with moderately buckled bars without the need of previously repairing the reinforcement bars, an application technique which may considerably facilitate the retrofit of earthquake damaged RC columns. Factors for the estimation of the reduced mechanical properties of the repaired specimens compared to the respective values for intact CFRP-jacketed specimens, in relation to the level of damage prior to retrofit, are proposed both for the compressive strength and the average modulus of elasticity. It was determined that the compressive strength of the retrofitted CFRP-jacketed columns is reduced by 90% to 65%, while the average modulus of elasticity is lower by 60% to 25% in respect to similar undamaged columns jacketed with the same layers of CFRP.

**Keywords:** axial compressive strength; buckling of longitudinal bars; damage level; retrofit with CFRP jacket; short reinforced concrete column; stiffness and ductility

## 1. Introduction

Reinforced concrete (RC) buildings in seismic regions constructed before 1980's were typically non-ductile frame structural systems designed for gravity loads with inadequate reinforcement detailing, factors that render those buildings vulnerable to future earthquakes. Insufficient transverse reinforcement and confinement of old-type RC columns are typical reinforcement inadequacies liable to result in shear failure and buckling of the longitudinal reinforcement in the event of a major earthquake (Tena-Colugna *et al.* 2022).

Numerous studies have explored techniques for seismic strengthening of substandard RC structural elements as a preventive measure against future earthquakes (among others Pampanin *et al.* 2007, Karayannis *et al.* 2008, Tsonos 2008, Kalogeropoulos *et al.* 2016 and 2019a, Ding *et al.* 2018, Kalogeropoulos and Tsonos 2019, Kahn *et al.* 2022). Externally applied fiber-reinforced polymer (FRP) jackets have proved to be effective in enhancing the axial strength and ductility of RC columns with insufficient transverse reinforcement (Deamers and Neale 1999, Tastani *et al.* 2006, Ozcan *et al.* 2008, Rousakis and Karabinis 2008 and 2012, Ilki *et al.* 2018, Carillo *et al.* 2020, Elci 2020) and

also in reducing the risk of buckling of rebars (Giamundo *et al.* 2014, Pantazopoulou *et al.* 2016, Bai *et al.* 2017).

Furthermore, FRP jacketing is effective for the retrofit of RC columns which have suffered damage, both in the presence of small to medium level of pre-existing damage (e.g., Wang *et al.* 2012, Faustino and Chastre 2016, Karayannis and Golias, 2018), but also in heavily damaged columns (e.g., Saadatmanesh *et al.* 1997, Cheng *et al.* 2003, Sami *et al.* 2022). In case of buckled longitudinal reinforcement, the rebars are usually straightened prior to retrofitting (e.g., Saiidi and Cheng, 2004, He *et al.* 2013). The advantage of applying continuous CFRP jackets instead of alternative retrofit techniques in considerably speeding up the rehabilitation of damaged RC columns has been underlined also by Vosoghi and Saiidi (2012 and 2013).

The present paper deals with short RC columns with insufficient transverse reinforcement which have often been reported to trigger collapse of older RC buildings worldwide (see Fig. 1) (Moretti 2008, Kam *et al.* 2011, Ricci *et al.* 2011, Vicente *et al.* 2012). CFRP jacketing has been effectively applied as a retrofit technique of short RC columns with inadequate transverse reinforcement (Jin *et al.* 2020, Dirikgil 2021, Bedirhanoglu *et al.* 2022) and may shift the mode of failure from shear to flexural (Kargaran and Kheyroddin 2020). It is noted that for lower aspect ratios,  $L/h$  (see Fig. 2), the governing shear transfer mechanism in RC columns is the strut, which results in column expansion at mid-height and subsequent explosive shear failure along the main diagonals (Yamada and Furui

\*Corresponding author, Associate Professor  
E-mail: moretti@central.ntua.gr



Fig. 1 Failure of short RC columns at the 1999 earthquake in Athens

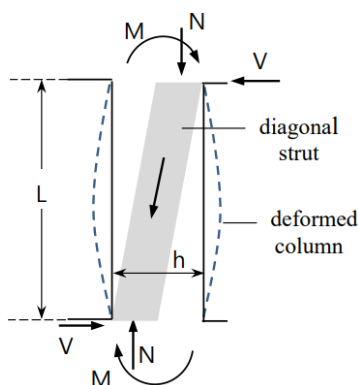


Fig. 2 Dominant load transfer mechanism for double-fixed short columns subjected to lateral loading

1968, Moretti and Tassios 2006, 2007 and 2013). Hence, the FRP jacket in a similar short RC column is liable to deform more and, therefore, be more effective in providing confinement at mid-height, as compared to the lower activation of FRP in case of a confined flexural hinge of a long column (Zhiguo *et al.* 2017). This issue has not been previously brought up to the best knowledge of the author.

This study was aimed at developing a rapid and efficient repair procedure for substandard short RC columns with moderately buckled longitudinal bars without previously intervening in the buckled part of the bar using CFRP jacketing. It is noted that in the typical repair practice of concrete jacketing the buckled part of the old bar is cut and its two ends are butt- or lap-welded to a new piece of steel bar (Fardis 2009, Kalogeropoulos *et al.* 2019b). However, this technique may not be apposite for older structures in which non-weldable cold-rolled steel was used.

The experimental results of substandard RC column models tested until reaching different damage states, subsequently repaired by CFRP jacketing and re-tested until failure are discussed. Although the columns are subjected to axial compression, the conclusions drawn from this study are expected to be also applicable to short RC columns with shear ratio  $a_s < 1.0-1.5$  subjected to lateral loading, because of the similarity of deformation (where  $a_s = M/Vh$  with  $M$ ,  $V$  = moment and respective shear force and  $h$  = section dimension parallel to  $V$ ) (Fig. 2).

## 2. Experimental program

### 2.1 Overview

Twelve 1/3-scale physical short column models, with inadequate transverse reinforcement and reinforcement properties typical of RC buildings constructed in Greece prior to 1990s, were subjected to monotonic compression up to failure. Furthermore, six control CFRP-jacketed specimens, three with and three without steel reinforcement, were also tested. A scale of damage ranging from I to V is proposed, focusing on the extent of rebar buckling, according to which the damage level of the tested specimens was assessed. Subsequently to the first testing, 10 specimens with variable degree of damage were selected, retrofitted using cementitious mortar and CFRP jacketing, and were re-tested in compression. The number of CFRP layers in the jacket was estimated from the level of damage allocated after the first test, and was kept to the minimum required to guarantee a damage level in the second test similar to that initially observed. A length scale factor of  $S_L = 3$  was generally followed (dimensions and material characteristics, i.e., longitudinal rebars, stirrups, and concrete mix) which renders more reliable the extrapolation of results to 1/1 scale.

### 2.2 Specimens' characteristics

RC columns with height 300 mm and three different sections, i.e., round with 150 mm diameter, and square with side of 100 mm and 150 mm and corners chamfered with a radius  $R_c = 25$  mm, were constructed and tested under concentric compression. The reinforcement cage was detailed so as to represent the detailing practices in older Greek buildings. The transverse ties are closed at 135 degrees, contrary to the older practice of 90-deg, with the intention to avoid opening of the stirrups and early buckling of the longitudinal rebars. Clear concrete cover was generally  $c = 7$  mm. The longitudinal reinforcement consists of  $\varnothing 6$ -mm rebars, with reinforcement ratio slightly over 1%, while the transverse reinforcement consists of a 3-mm closed stirrup at the outer perimeter of the longitudinal bars.

The specimen geometry and reinforcement layout are displayed in Figs. 3-4. Scaling 1/3 has been generally observed, i.e., in geometry, reinforcement and concrete mix.

In general specimens have center-to-center distance,  $s$ , between consecutive stirrups equal to 70 mm ( $\varnothing 3@70$ ), conforming to the practice in Greece until 1985.

For each cross section one specimen was manufactured with stirrups spaced at 45.5 mm ( $\varnothing 3@45.5$ ) which results to a ratio of stirrup spacing,  $s$ , to longitudinal bar diameter,  $d_b$ ,  $s/d_b = 7.6$ .

Among other codes, Eurocode 8 (2004) reports that, for moderate level of ductility, for ratios  $s/d_b \leq 8$  there is no risk of buckling of the longitudinal reinforcement. For the columns with stirrups  $\varnothing 3@70$  the respective ratio is  $s/d_b = 11.7$ , which renders them vulnerable to buckling.

The testing program was performed (a) to specimens without previous damage (henceforth called "intact" or "undamaged") and (b) to specimens previously damaged

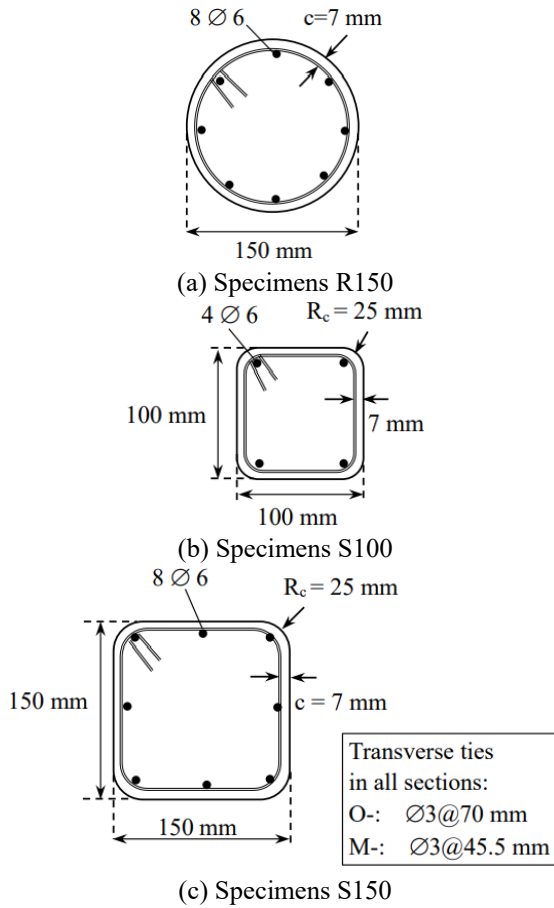


Fig. 3 Reinforcement layout of tested columns

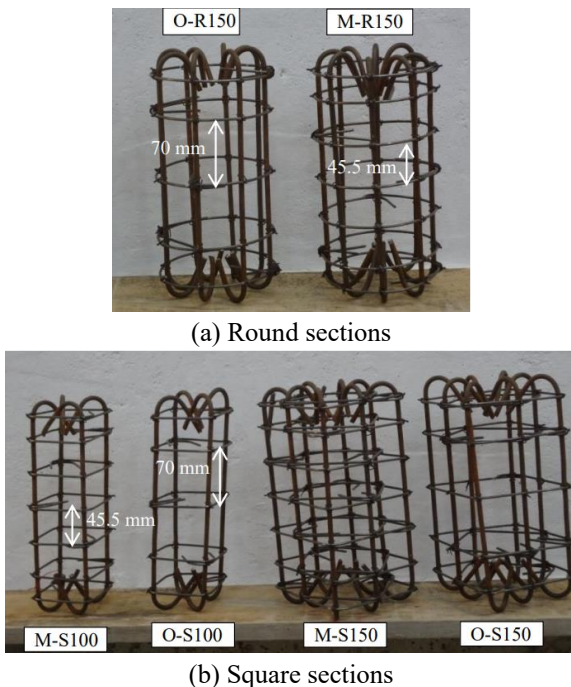


Fig. 4 Reinforcement cages of specimens

Specimen names feature their particular characteristics, as follows: First letter O- or M- corresponds, respectively, to stirrups  $\text{Ø}3@70$ , encountered in older (O) structures and to stirrups  $\text{Ø}3@45.5$ , in line with modern (M) code provisions. Consecutively, R150 indicates a round (R) section with 150 mm diameter, while S100 and S150 refer to square (S) section with side 100, 150 mm, respectively. Following symbols (C) or -1C equally indicate the presence of 1-layer CFRP jacket. Suffix “str” indicates the presence of 70-mm CFRP strips at both ends of a column aiming at preventing concrete failure due to local anchorage stresses. Illustratively, O-S150str refers to a column with stirrups  $\text{Ø}3@70$ , square cross section with side 150 mm, and reinforced at the ends by strips of 70-mm height.

Repaired specimens are designated by prefix “r-” and a suffix that indicates the number of CFRP layers used for retrofit, e.g., specimen r-O-R150(C)-2C is a 150 mm-diameter column, with stirrups  $\text{Ø}3@70$ , with 1-layer initial CFRP-jacket that was repaired by 2 layers of CFRP jacket.

Three control cylindrical columns without steel reinforcement (UR150-) wrapped with 1, 2, and 3 CFRP layers were also tested.

### 2.3 Materials

Concrete mix was manufactured in the laboratory with 1/3 scaled-down aggregates. Proportioning of aggregates by weight was 20.8% (4-8-mm), 19.1% (2-4-mm), 14.4% (1-2-mm), 13.6% (0.5-1-mm) and 12% (<0.5-mm).

Columns with square sections were cast horizontally in wooden molds, while cast-iron molds were used for the circular columns. All specimens were cast on the same day, but were tested in two different time periods. Unconfined concrete compressive strength,  $f_{co}$ , was determined on plain concrete cylinders at the period of testing, as 22.98 MPa and 27.30 MPa for the two respective groups of specimens.

Longitudinal rebars consist of smooth mild steel which was typically used in older structures in Greece, with yield strength 350 MPa and yield strain 0.00175. Transverse reinforcement consists of smooth wire with yield strength 560 MPa. It is noted that the high yield strength of the wire does not affect the results, given that the objective was to observe the rebar scaling 1/3 and to study rebar buckling.

FRP jackets are unidirectional carbon fiber tow sheets with thickness  $t_f=0.129$  mm/ply, tensile strength 4300 MPa, elastic modulus 230 GPa and 1.7% ultimate tensile strain.

### 2.4 Application process of CFRP jackets

CFRP jackets were applied (a) on intact columns through dry lay-up process and (b) on the repaired pre-damaged columns through wet lay-up process for better bonding at the overlap length.

In damaged specimens crushed concrete and loose particles were removed, an epoxy bonding agent was applied on the concrete substrate, the damaged concrete was replaced by fiber reinforced cement-based repair mortar (with compressive strength 45 MPa and minimum tensile strength 8 MPa) and the CFRP jacket was applied. Material technical properties are available in Moretti *et al.* (2021a).

and subsequently retrofitted by the application of one to three layers of CFRP jacket (hereafter referred to as “retrofitted” or “repaired”).

Table 1 Experimental data of the specimens

Specimen	$P_{max}$ (kN)	$f_{co}$ (MPa)	$\varepsilon_{cu,max}$ (‰)	$\varepsilon_{lu,max}$ (‰)	$E_{cm}$ (MPa)	$E_{c,eff}$ (MPa)	Area [ $\sigma$ - $\varepsilon$ ] (MPa)
O-S100(C)	450	22.98	-21.22	9.67	21030	804	803
O-S100	287	22.98	-1.22	0.16	39420		29
M-S100	298	22.98	-1.41	0.24	36508		33
O-S150(C)	770	22.98	-15.63	n.a <sup>(2)</sup>	25036	n.a <sup>(2)</sup>	387
O-S150	572	22.98	-3.28	2.04	21275		65
M-S150	623	22.98	-3.15	1.37	31503		98
O-R150(C)	772	22.98	-23.24 <sup>(1)</sup>	14.37	16491 <sup>(1)</sup>	817 <sup>(1)</sup>	779 <sup>(1)</sup>
O-R150	416	22.98	-2.85 <sup>(1)</sup>	2.66 <sup>(1)</sup>	23553 <sup>(1)</sup>		51 <sup>(1)</sup>
M-R150	441	22.98	-5.47 <sup>(1)</sup>	7.81 <sup>(1)</sup>	23796 <sup>(1)</sup>		112 <sup>(1)</sup>
O-S100str	332	27.30	n.a <sup>(2)</sup>	n.a <sup>(2)</sup>	27040		84
O-S150str	697	27.30	n.a <sup>(2)</sup>	n.a <sup>(2)</sup>	27260		45
O-R150str	516	27.30	n.a <sup>(2)</sup>	n.a <sup>(2)</sup>	19987 <sup>(1)</sup>		310 <sup>(1)</sup>
O-S100-1C	463	27.30	-8.64	10.44	27129	1507	339
O-S150-1C	886	27.30	-12.42	13.45	30362	476	199
O-R150-1C	802	27.30	-20.27 <sup>(1)</sup>	13.20	34889 <sup>(1)</sup>	809 <sup>(1)</sup>	736 <sup>(1)</sup>
UR150-1C	720	27.30	-23.17 <sup>(1)</sup>	14.94	24730 <sup>(1)</sup>	694 <sup>(1)</sup>	720 <sup>(1)</sup>
UR150-2C	1148	27.30	-27.28 <sup>(1)</sup>	14.39	21540 <sup>(1)</sup>	1181 <sup>(1)</sup>	1304 <sup>(1)</sup>
UR150-3C	1259	27.30	-24.34 <sup>(1)</sup>	12.20	22157 <sup>(1)</sup>	1482 <sup>(1)</sup>	1238 <sup>(1)</sup>
r-O-S100(C)-1C	495	27.30	-12.58	12.48	13084	1894	466
r-O-S100-1C	409	27.30	-12.94	8.96	23541	582	488
r-O-S150(C)-2C	965	27.30	-5.47	11.19	13615	5902	137
r-O-S150-1C	729	27.30	-7.38	8.63	14760	594	192
r-O-R150(C)-2C	988	27.30	-21.10 <sup>(1)</sup>	11.00	9577 <sup>(1)</sup>	1169 <sup>(1)</sup>	866 <sup>(1)</sup>
r-O-R150-3C	1325	27.30	-32.98 <sup>(1)</sup>	15.35	7979 <sup>(1)</sup>	1142 <sup>(1)</sup>	1503 <sup>(1)</sup>
r-M-R150-3C	1161	27.30	-28.43 <sup>(1)</sup>	12.31	7974 <sup>(1)</sup>	1355 <sup>(1)</sup>	1270 <sup>(1)</sup>
r-O-S100str-1C	510	27.30	-13.30	15.10	9553	1912	358
r-O-S150str-2C	974	27.30	-16.40	11.47	9421	1140	513
r-O-R150str-2C	1216	27.30	n.a <sup>(2)</sup>	16.84	7449 <sup>(1)</sup>	980 <sup>(1)</sup>	n.a <sup>(2)</sup>

Notation: <sup>(1)</sup> from LVDT measurements (else from strain gage measurements), <sup>(2)</sup> not available.

$P_{max}$ : Maximum Axial Load at Test;  $f_{co}$ : Compressive Cylinder Concrete Strength,  $\varepsilon_{cu,max}$  (‰): Axial Strain at Maximum Load,  $\varepsilon_{lu,max}$  (‰): Lateral Strain at Maximum Load,  $E_{cm}$ : Average Modulus of Elasticity (Fig.14),  $E_{c,eff}$ : Effective Modulus of Elasticity (Fig.14), Area [ $\sigma$ - $\varepsilon$ ] as displayed in Fig. 14

Additional 35-mm height CFRP strips were placed at both ends, externally to the jacket, to constrain the location of FRP rupture to the middle section (Lam and Teng 2004, Lim and Ozbakkaloglu 2015).

The overlap length in the CFRP jackets was 150 mm, increased by 30% to avoid debonding (Moretti and Arvanitopoulos 2018). In the square cross-sections overlap was performed at corners (e.g., Moretti 2019). Multilayered jackets were applied as a continuous sheet. FRP jackets were cured for at least seven days according to manufacturer's guidelines.

### 2.5 Instrumentation

Lateral and axial strains of the CFRP jackets were recorded through 20-mm unidirectional strain gages. In specimens with round section strains were also measured by

linear variable displacement transducers (LVDTs), which were attached on a Humboldt metallic testing frame. LVDTs record the average axial strain over 203-mm length at mid-height, and the lateral strains along the diameter at the middle of each column.

### 3. Test results and discussion

The specimens were tested under monotonic axial compression. Unidirectional strain gages located outside the overlap length of the FRP jacket were used to record the axial and lateral strains at mid-height. Additionally, in the circular columns lateral and axial deformations were measured by linear variable displacement transducers (LVDTs). Table 1 summarizes the characteristic experimental values, including the maximum compressive

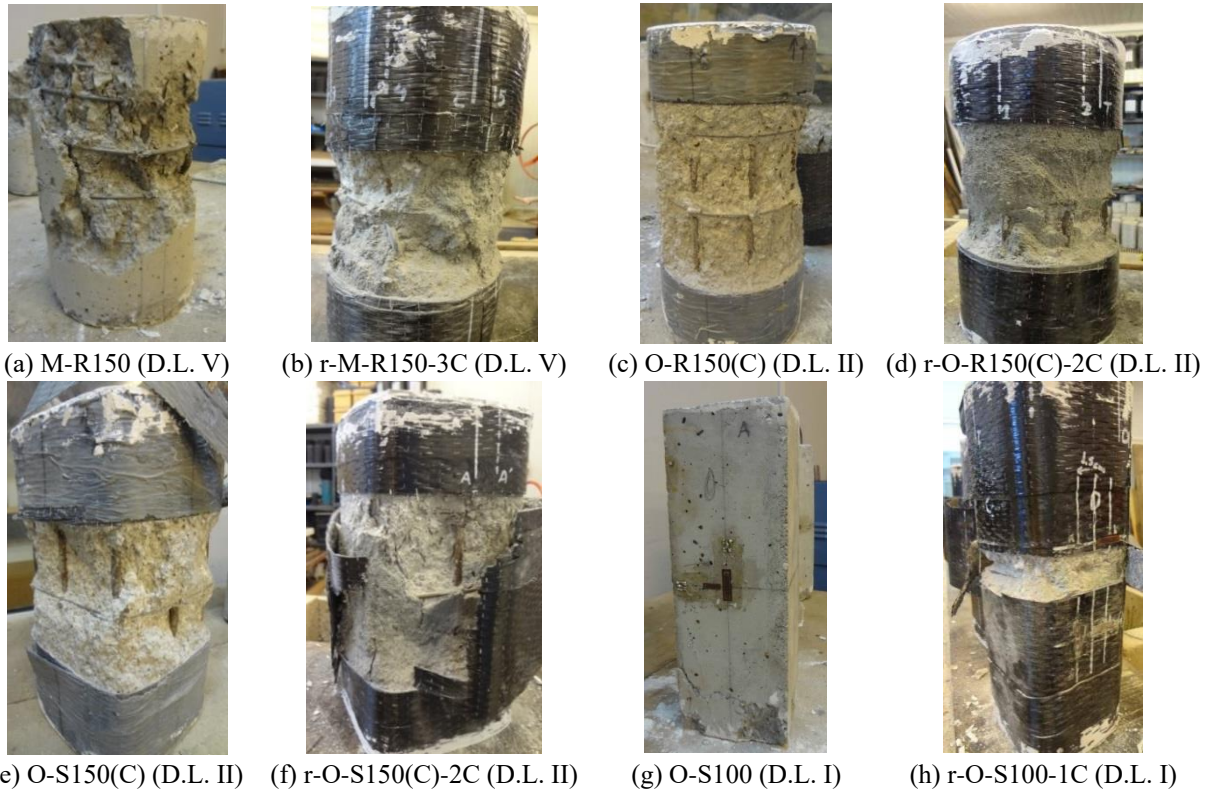


Fig. 5 Damage after testing of intact (first test) and of the respective repaired columns (prefix r-) at second test. The respective damage level (D.L.) allocated according to Table 2 is indicated in parenthesis

load,  $P_{max}$ , the axial strain  $\varepsilon_{cu,max}$  and the lateral strain  $\varepsilon_{lu,max}$  at load  $P_{max}$  and the unconfined compressive cylinder concrete strength  $f_{co}$ .

### 3.1 Mode of failure

Square RC columns failed prematurely at the ends, owing to stress concentration (Fig. 5(g)), which was prevented by adding 70-mm CFRP strips at column ends (which is indicated by suffix “str” in the specimens’ name). In circular columns such failure did not occur, and loading continued after peak axial load so as to obtain different levels of damage to use in the retrofit scheme (e.g., Fig.5(a)).

The CFRP jacket ruptured outside the overlap length. More particularly, in columns with square section the jacket typically ruptures in the region of the corners where higher stress concentrations are expected as shown in Fig. 5(f).

It was generally observed that buckled bars along which the crushed concrete was replaced by repair mortar were less liable to buckling than the bars which remained encased in the original concrete at the end of the first test. It is noted that in most cases the repair mortar did not even spall (Figs. 5(d) and (f)). Hence, it appears that the presence of repair mortar with higher strength than the original concrete may result in improved restraint against lateral dilation of the concrete core, as established also by Tastani *et al.* (2006).

Based on visual observations, buckled reinforcement does not seem to have significantly precipitated the rupture

Table 2 Description of damage levels (D.L.)

D.L.	Damage observed
	$d \leq 1$ mm
I	Insignificant spalling of concrete Limited exposure of reinforcement
	$1 \text{ mm} < d \leq 3$ mm
II	Concrete spalling Revelation of longitudinal bars
	$3 \text{ mm} < d \leq 5$ mm
III	Concrete crushing Extensive exposure of longitudinal bars
	$5 \text{ mm} < d \leq 10$ mm
IV	Widespread concrete crushing None or slight tilting/ distortion
	$5 \text{ mm} < d \leq 15$ mm
V	Widespread concrete crushing Substantial tilting/ distortion

Notation:  $d$ : Maximum Deflection from verticality of longitudinal bars because of buckling

of the CFRP jacket in contrast to what has been claimed by Tastani *et al.* (2006) and Bournas and Triantafillou (2011) among others. It rather appears that buckling of longitudinal bars followed the rupture of FRP jacket, as Deamers and Neale (1999) concluded from full-scale tests.

### 3.2 Damage assessment

Classification of structural damage is typically adopted in codes for seismic assessment and retrofit design (C.E.B 1983, KAN.EPE 2012, ATC-32 1996, JBDPA 1991), and in

Table 3 Experimental data of the specimens and predicted strengths of the retrofitted specimens

Intact Specimens	$f_{cc,exp}/f_{co}$	D.L.	Retrofitted Specimens	$f_{cc,exp}/f_{co}$	D.L.	$f_{cc,exp}$ (MPa)	$f_{cc,anal}$ (MPa)	$f_{cc,exp}/(R_{fcc}f_{cc,anal})$
O-S100(C)	2.07	I	r-O-S100(C)-1C	1.91	I	52.3	43.86	1.25
O-S100	1.32	I	r-O-S100-1C	1.58	I	43.2	43.86	1.04
O-S150(C)	1.53	II	r-O-S150(C)-2C	1.61	II	43.9	42.29	1.22
O-S150	1.13	II	r-O-S150-1C	1.22	II	32.4	36.74	1.06
O-R150(C)	1.90	II	r-O-R150(C)-2C	2.05	II	55.9	65.46	1.00
O-R150	1.02	IV	r-O-R150-3C	2.75	IV	75	82.26	1.22
M-R150	1.09	V	r-M-R150-3C	2.41	V	65.7	83.36	1.13
O-S100str	1.29	II	r-O-S100str-1C	1.97	II	53.9	43.86	1.45
O-S150str	1.16	II	r-O-S150str-2C	1.62	II	44.3	42.29	1.23
O-R150str	1.07	III	r-O-R150str-2C	2.52	IV	68.8	65.46	1.31

$f_{cc,exp}$ : Maximum Experimental Axial Strength,  $f_{co}$ : Compressive cylinder Concrete Strength,  $f_{cc,anal}$ : Predicted Axial Strengths from Eqs. (1)-(3),  $R_{fcc}$ : Reduction Factors for the pre-damaged specimens (Table 4)

post-earthquake damage assessment (ATC-20 1991, Anagnostopoulos and Moretti 2008). However, damage criteria vary considerably between different code provisions and individual studies (e.g., Mesbah and Benzaid 2017, Wang *et al.* 2022).

Based on the experimental observations, a damage scale of increasing damage severity ranging from I to V, is proposed as shown in Table 2. The classification of damage focusses on the extent of buckling of longitudinal bars and includes damage in concrete and distortion of specimen.

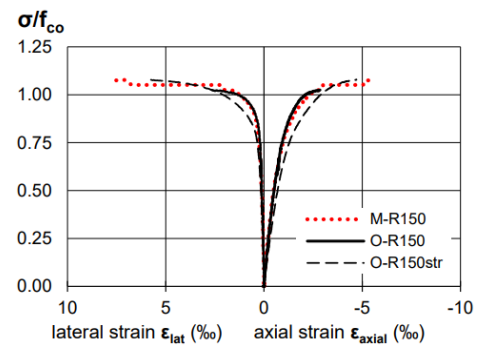
After the first test, the damage of the RC columns that would be repaired was meticulously recorded and a damage level (D.L) was allocated according to Table 2.

The number of CFRP plies for retrofit was estimated so that each repaired specimen at re-testing would exhibit similar level of damage and no further buckling of the longitudinal bars in respect to the original specimen. Table 3 displays, in one row for each specimen, the values D.L for the intact and for the respective retrofitted specimen. With the exception of specimen O-R150str, the repaired specimens had the same damage level as the initial ones, hence the retrofit may be considered as sufficient. It is noted that 1 layer of CFRP jacket corresponds to volumetric FRP ratio,  $\rho_f$ , equal to 0.34% for columns R150 and S150, and to 0.52% for columns S100.

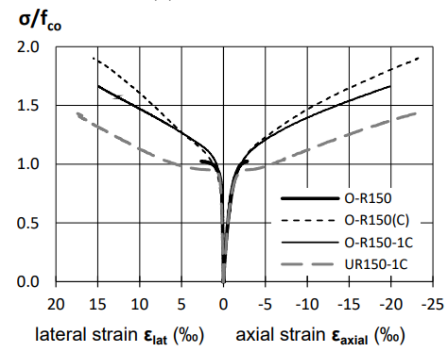
### 3.3 Stress-strain experimental behavior

RC columns with closer spaced ties ( $\varnothing 3@45.5$ , M-specimens) had 4-8% higher peak compressive strength and increased deformation at maximum load, compared to O-specimens ( $\varnothing 3@70$ ), as shown in Fig. 6(a) for columns with circular section. The presence of 7-cm-wide CFRP strips, at both ends of O- specimens resulted in a slightly improved axial behavior for specimen O-R150str compared to specimen O-R150 (Fig. 6(a)).

One layer of CFRP jacketing in O- specimens results in 70-80% increase in axial strength and more than 500% increase in respective lateral and axial deformation. Hence, CFRP jacketing is effective in upgrading the seismic performance of short columns with insufficient transverse



(a) RC columns



(b) with one CFRP layer

Fig. 6 Stress-strain curves for columns with round section not previously damaged (strains from LVDTs)

reinforcement. Plain concrete specimen UR150-1C with 1 CFRP layer displayed similar maximum strains but reduced axial strength compared to the respective reinforced specimens (Fig. 6(b)).

Fig. 7 to 9 display the axial stress,  $\sigma$ , against axial ( $\epsilon_{axial}$ ) and lateral ( $\epsilon_{lat}$ ) strain diagrams for repaired specimens with the three section types. Strains from LVDTs are typically higher than respective local strains measured from strain gages (s.g.) in case of specimens with round sections for which both measurements are available as depicted in Fig. 7 (see also Moretti *et al.* 2021a). It is interesting to note that in specimen r-O-R150(C)-2C (Fig. 7), in which s.g. 4 was located in the region where a longitudinal rebar suffered

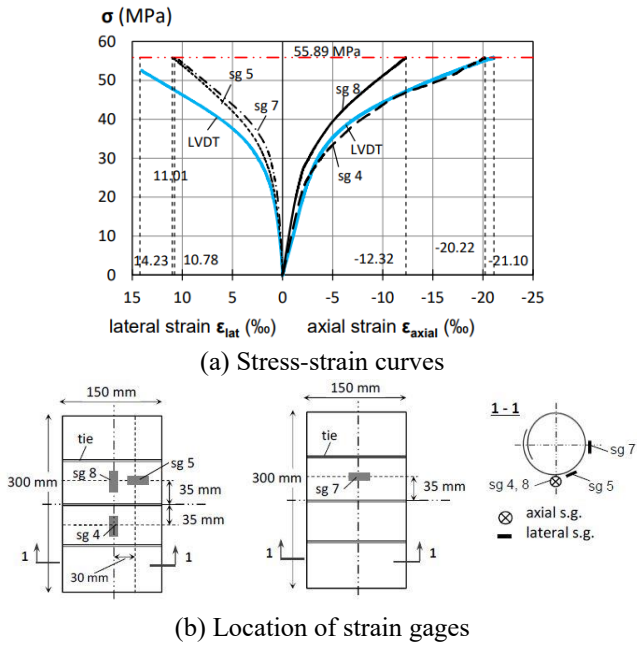


Fig. 7 Specimen r-O-R150(C)-2C

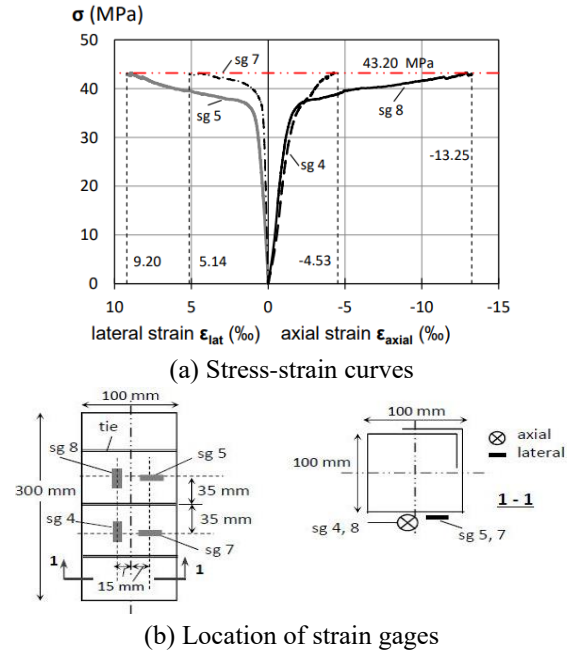


Fig. 9 Specimen r-O-S100-1C

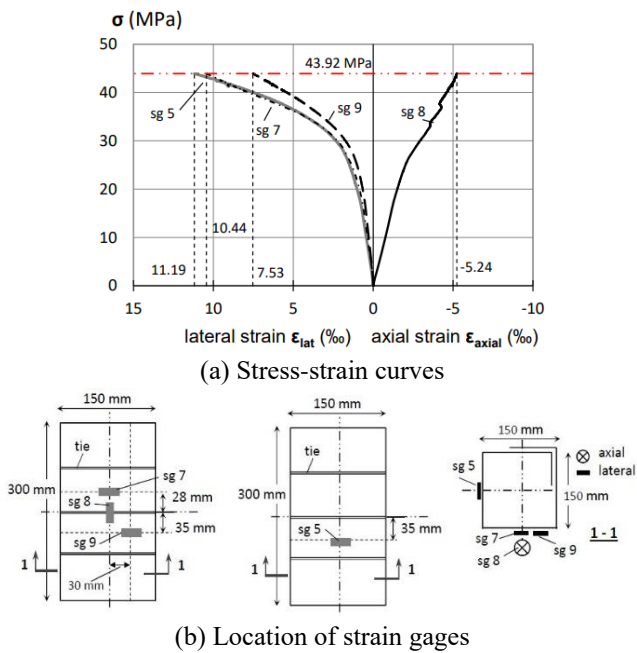


Fig. 8 Specimen r-O-S150(C)-2C

buckling, axial strains from the LVDT were similar to those measured from s.g. 4, which indicates that the global axial deformation corresponded to local buckling. The magnitude of local lateral strains  $\epsilon_{lat}$  does not seem to depend on whether they are measured on a longitudinal rebar or away from the rebar (Figs. 7, 8), but is rather influenced by whether the strain gage is located in a region of stress localization which gives rise to rupture of the FRP jacket.

In Fig. 9 (specimen r-O-S100-1C) it may be observed that strains measured in locations in which the FRP jacket did not rupture, i.e., s.g. 4 and s.g. 7, were typically lower than respective strains in parts where the jacket ruptured, i.e., s.g. 8 and s.g. 5. The difference in respective axial and

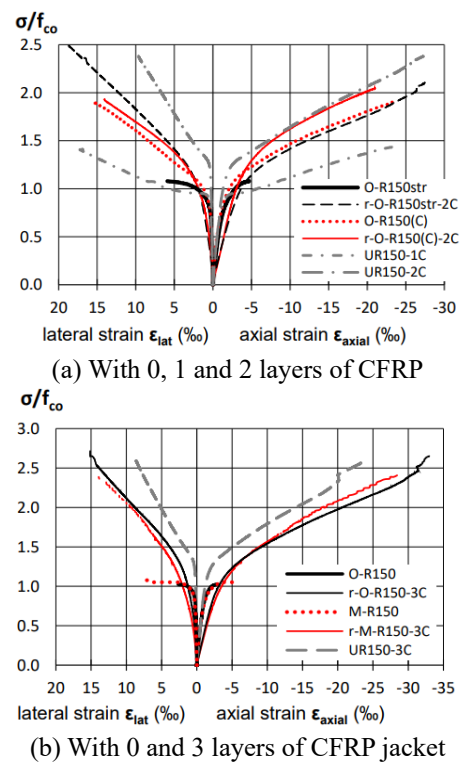


Fig. 10 Axial stress - strain diagrams of intact and retrofitted specimens with round section (strains measured by LVDTs)

lateral strains was observed for stresses immediately above the unconfined concrete strength,  $f_{co}$ , which may imply that local deformations and stress concentration which finally led to rupture of the jacket were already present in that part of the specimen at the beginning of activation of the FRP jacket.

Figs. 10 and 11 depict the axial stress,  $\sigma$ , normalized

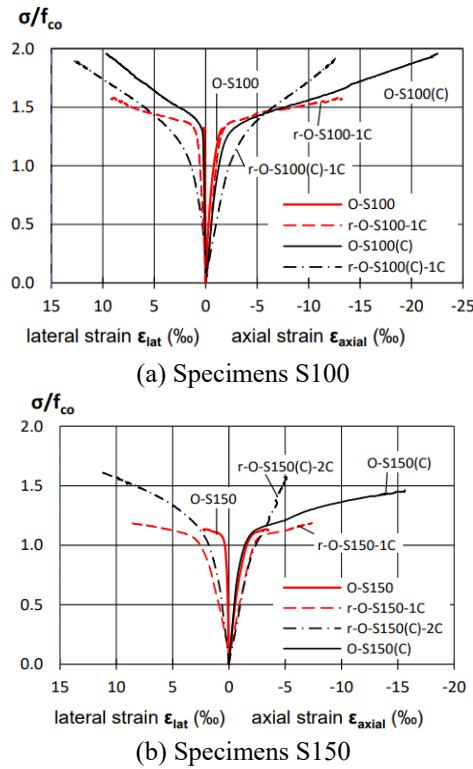


Fig. 11 Axial stress - strain diagrams of intact and retrofitted specimens with square section (strains from strain gages)

with the compressive cylindrical concrete strength,  $f_{co}$ , versus axial and lateral strain,  $\varepsilon$ , diagrams. Intact specimens jacketed or not, show similar initial stiffness for axial stresses lower than the unconfined concrete strength,  $f_{co}$ , i.e., before the activation of the FRP jacket. Repaired specimens with pre-existing damage have reduced initial stiffness compared to the respective intact ones (e.g., Fig. 10(b): O-R150 and M-R150, vs. the respective retrofitted specimens r-O-R150-3C and r-M-R150-3C). However, the stiffness of the retrofitted columns after the activation of the FRP jacket does not seem to be significantly affected by the extent of pre-existing damage, as may be observed by comparison, e.g., between O-R150(C) and r-O-R150(C)-2C in Fig. 10(a). The modulus of elasticity before and after the activation of the FRP jacket of the columns is calculated according to experimental measurements in section 4.2.

The longitudinal reinforcement bars increase the axial compressive strength of the intact RC columns, as shown in Fig. 6(b) by comparing specimens UR150-1C (unreinforced) and O-R150-1C. However, the contribution of the longitudinal reinforcement decreases in the retrofitted specimens in which the longitudinal rebars were buckled prior to retrofitting, as may be observed in Figs 10(a) and 10b, by comparing the unreinforced specimens UR150-2C and -3C with other specimens retrofitted by the same number of CFRP layers.

#### 4. Mechanical properties of retrofitted specimens

Higher damage level (D.L.) of pre-existing damage

results, in general, in lower peak axial stress and increased deformations of the retrofitted specimens compared to the intact, if the same layers of CFRP jacket are used, e.g., in Fig. 10(b): columns r-O-R150-3C (initial D.L. IV) and r-M-R150-3C (initial D.L. V).

For the seismic capacity assessment of a repaired damaged structural element, a safe estimation of its mechanical characteristics is required. To this purpose, a methodology will be adopted which is often applied for the estimation of the residual mechanical properties of earthquake damaged RC structural elements: Reduction factors,  $R$ , are introduced by which the mechanical properties of the intact structural element are multiplied in order to obtain the respective properties of the damaged specimen, e.g., Maeda *et al.* (2014), Kono *et al.* (2011). Based on the experimental results, reduction factors,  $R$ , for the estimation of the axial strength and average modulus of elasticity of the repaired columns in relation to the respective properties of the intact columns, for D.L. I to V, are proposed.

##### 4.1 Estimation of axial strength

Peak axial confined compressive strength,  $f_{cc}$ , is typically related to lateral confinement pressure. In this study, the confined axial strength,  $f_{cc}$ , is calculated according to Eqs. (1)-(3). Details of the design model, which is based on the Eurocodes (Eurocode 2 2004, Eurocode 8 2004, and Eurocode 8 2005) is available in Moretti *et al.* (2021b).

$$f_{cc} = f_{co} \left( 1.0 + 5.0 \cdot \frac{\sigma_2}{f_{co}} \right) \text{ for } \sigma_2 \leq 0.05 f_{co} \quad (1a)$$

$$f_{cc} = f_{co} \left( 1.125 + 2.5 \cdot \frac{\sigma_2}{f_{co}} \right) \text{ for } \sigma_2 > 0.05 f_{co} \quad (1b)$$

$$\sigma_2 = f_{l,f} + f_{l,st} \quad (2)$$

$$f_{l,f} = \frac{2 \cdot \varepsilon_{fu} \cdot E_f \cdot t_f}{D} \quad (3)$$

where  $f_{co}$  is the cylinder compressive strength of the unconfined concrete,  $\sigma_2$  is the total lateral stress from Eq. (2),  $f_{l,f}$  is the lateral pressure from the FRP jacket according to Eq. (3),  $f_{l,st}$  is the lateral stress from stirrups calculated according to Eurocode 8 (2004),  $\varepsilon_{fu}$  is the FRP strain at failure provided by the manufacturer,  $E_f$  is the FRP elastic modulus,  $t_f$  is the total thickness of the FRP jacket, and  $D$  is the diameter in case of a circular cross-section, or the larger cross-section width in case of rectangular cross-sections.

The use of tensile strain,  $\varepsilon_{fu}$ , of the FRP fabric in Eq. (3) -and not of a reduced FRP ultimate strain as proposed in other design models, e.g., in Eurocode (2005), is aimed at overcoming the uncertainty involved in the estimation of the FRP lateral strain at failure (Moretti *et al.* 2021b).

Effectiveness factors, in the plane of the section and along the height, are used for the calculation of lateral pressures both for FRP and stirrups.

The longitudinal reinforcement is not included in the calculation of the axial strength. This assumption is in accordance to the observation made in the present study that

Table 4 Minimum required volumetric ratio  $\rho_{f,min}$  of CFRP and reduction factors  $R$  of mechanical properties for the repaired columns related to the initial damage level (D.L.)

D.L.	$d$ (mm)	$\rho_{f,min}$	$R_{fcc}$	$R_{Ecm}$
I	$d \leq 1$ mm	0.3	0.90	0.60
II	$1 \text{ mm} < d \leq 3$ mm	0.5	0.85	0.50
III	$3 \text{ mm} < d \leq 5$ mm	$> 0.7$	0.80	0.25
IV	$5 \text{ mm} < d \leq 10$ mm	1	0.75	0.25
V	$5 \text{ mm} < d \leq 15$ mm and distortion	1	0.65	0.25

Notation:  $d$ =deflection of rebars from verticality because of buckling,  $\rho_{f,min}$ =minimum required volumetric ratio of CFRP so that no further buckling occurs,  $R_{fcc}$ ,  $R_{Ecm}$ =Reduction factors for axial strength and average modulus of elasticity.

with increasing amount of rebar buckling (which is reflected by higher damage levels: D.L.>I) the contribution of longitudinal rebars to axial strength reduces, as discussed in section 3.3.

Table 3 displays the peak experimental compressive strength of the specimens  $f_{cc,exp}$  ( $=P_{max}/\text{area of section}$ , where  $P_{max}$  is displayed in Table 1), divided by the respective compressive strength of plain concrete,  $f_{co}$ , both for the intact and for the retrofitted columns. Table 3 displays also the predicted axial strengths from Eqs. (1)-(3),  $f_{cc,anal}$ , for the retrofitted columns. Table 3 includes also the values of damage level (D.L.) estimated according to Table 2, at the end of test both for the intact and for the retrofitted specimens.

It may be observed that for the retrofitted specimens the analytically calculated compressive strength overestimates the respective experimental strength ( $f_{cc,anal} > f_{cc,exp}$ ), with the overestimation increasing for increased damage level D.L. prior to the retrofit. This could be expected, because Eqs. (1) to (3) are intended for intact specimens.

It is proposed to estimate the confined axial strength of the retrofitted pre-damaged specimens,  $f_{cc,retrofitted}$  using Equ. (4), by multiplying  $f_{cc,anal}$  with a reduction factor  $R_{fcc}$  which considers the existing level of damage (D.L.). The proposed values of  $R_{fcc}$  are displayed in Table 4, and were calibrated against the test results so as to entail that the estimated axial strengths for the retrofitted specimens are safe. The ratio of experimental-to-predicted, according to Eq. (4), axial strength of the retrofitted columns ( $f_{cc,exp}/R_{fcc} \times f_{cc,anal}$ ) is displayed in the last column of Table 3.

$$f_{cc,retrofitted} = R_{fcc} \times f_{cc,anal} \quad (4)$$

Fig. 12 depicts for the circular columns, the average confinement pressure  $f_{l,aver}$  calculated from Eq. (3) at maximum axial load, using the average strain of all lateral strain gages, and the corresponding confined axial strength normalized by the cylinder concrete strength,  $f_{cc,exp}/f_{co}$ . It is observed that for the undamaged specimens UR150 both  $f_{l,aver}$  and  $f_{cc,exp}/f_{co}$  increase with increasing number of FRP layers. However, this relation is not so direct for the repaired specimens, because it depends also on the amount of pre-existing damage.

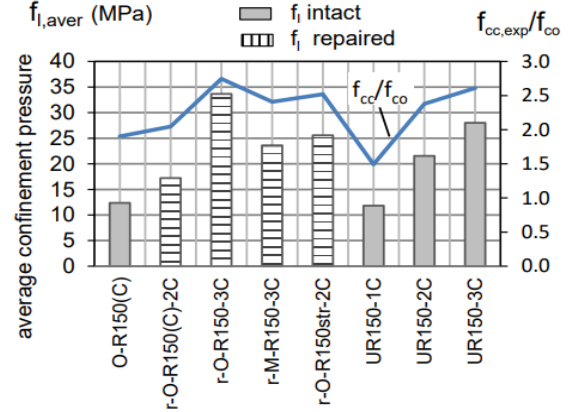


Fig. 12 Experimental axial strength  $f_{cc,exp}$  normalized to cylinder compressive strength  $f_{co}$ , and average confinement pressure  $f_{l,aver}$  according to strain gages for specimens with round section

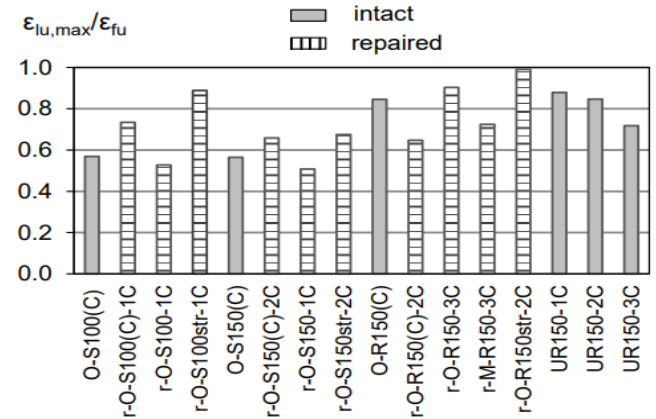


Fig. 13 Ratio of maximum hoop strain,  $\epsilon_{lu,max}$ , to rupture strain,  $\epsilon_{fu}$  provided by manufacturers for the CFRP

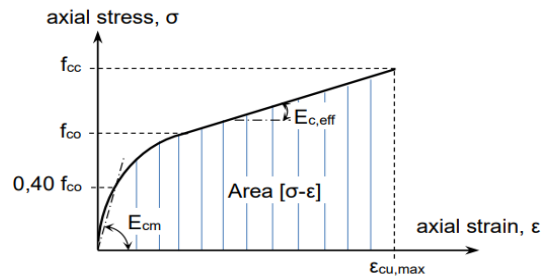


Fig. 14 Typical axial stress - strain diagram of FRP-jacketed specimen and designation of average and effective modulus of elasticity,  $E_{cm}$ , and  $E_{c,eff}$ , respectively

Fig. 13 displays the ratio of the maximum lateral strain  $\epsilon_{lu,max}$  measured from strain gages at maximum load to the ultimate CFRP tensile strain  $\epsilon_{fu}=1.7\%$  for the test specimens. In the retrofitted specimens, the values  $\epsilon_{lu,max}$  are subject to increased uncertainty as compared to the numerous uncertainties of intact specimens raised by Chen *et al.* (2010), among others.

#### 4.2 Initial elastic stiffness and dissipated energy

From the axial stress-axial strain diagrams the following

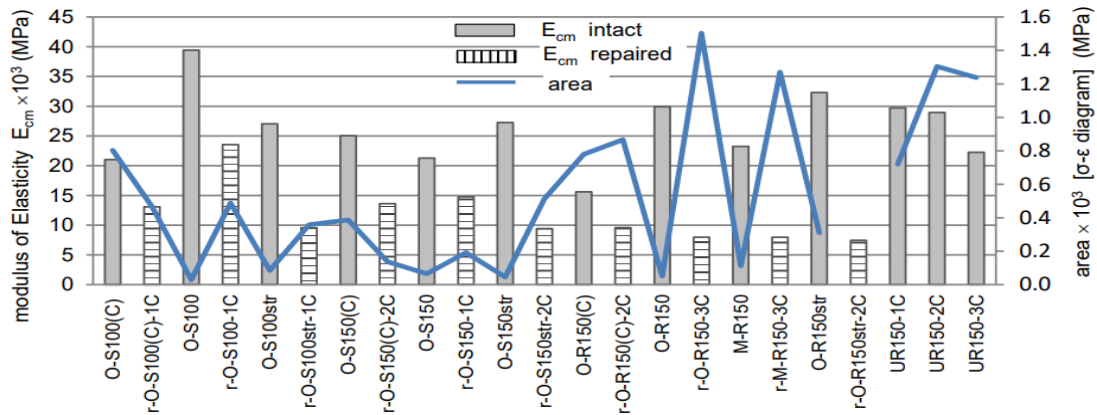


Fig. 15 Average modulus of Elasticity,  $E_{cm}$ , and area of stress-axial strain  $[\sigma-\varepsilon]$  diagram for the intact and the respective repaired specimens

values are calculated for the tested columns, as shown in Fig. 14: (a) the average modulus of elasticity,  $E_{cm}$ , from the tangent at a value of  $0.40f_{co}$ , where  $f_{co}$ =unconfined concrete cylinder compressive strength (Eurocode 2004) as an indicator of the initial stiffness prior to the activation of the FRP jacket, (b) the effective modulus of elasticity  $E_{c,eff}$  at the activation of the CFRP jacket, and (c) the area included in the  $[\sigma-\varepsilon]$  diagram up to failure, as an indicator of the energy dissipated and therefore, of ductility. Table 1 includes those three calculated values, when applicable (e.g.,  $E_{c,eff}$  is irrelevant for the unjacketed columns), for all specimens. Axial strains,  $\varepsilon_{axial}$ , are taken from LVDTs for round sections, and from maximum strain gage measurements for the square sections. It is noted that locally measured strains from strain gages are not so reliable, especially regarding the estimation of the area  $[\sigma-\varepsilon]$ .

Fig. 15 depicts the specimens' average modulus of elasticity,  $E_{cm}$  (left axis), and the area calculated from the  $[\sigma-\varepsilon]$  diagram (shown on the right axis). Both properties have an increased level of uncertainty and tend to decrease with increasing D.L. For the retrofitted specimens the value of  $E_{cm}$  does not seem to depend on the thickness of the FRP jacket, contrary to the area included in  $[\sigma-\varepsilon]$  diagram. Higher level of damage results in less area in the  $[\sigma-\varepsilon]$  diagram for the same number of CFRP layers (e.g., O-S100(C) compared to r-O-S100(C)-1C, and O-S150(C) compared to r-O-S150-1C).

Table 4 displays the proposed reduction factors,  $R$ , of the repaired RC columns for the axial strength,  $f_{cc}$ , and the average  $E_{cm}$  compared to intact columns, related to the damage level (D.L.) prior to retrofit. The minimum volumetric ratio,  $\rho_{f,min}$ , of CFRP jacket that proved to be apposite for the retrofit in relation to the initial value of D.L. so as to prevent further buckling is also included in Table 4. The findings of this work agree with Carillo *et al.* (2020) who concluded that CFRP jackets with  $\rho_f=0.5\%$  reduce the risk of rebar buckling in substandard square RC columns, irrespective of the spacing of transverse steel.

## 5. Conclusions

A methodology for the rapid retrofit of short RC

columns with sparsely spaced stirrups, including columns with moderately buckled longitudinal bars, using CFRP jacketing was explored. Although the tests were performed on columns subjected to axial loading, the derived results may be applied also to short RC columns with shear ratio  $a_s < 1.0-1.5$  subjected to lateral loading, because of the similarity of deformation at mid-height. Round and square sections, which benefit more from the CFRP lateral confinement, have been studied. Within the limitations of the test program the following conclusions were drawn:

- CFRP jacketing may be effectively used to upgrade the seismic performance of short columns with insufficient transverse reinforcement. In the present study one layer of CFRP jacket (i.e., volumetric FRP ratio equal to 0.34% for R150- and S150-, and 0.52% for S100-specimens) on intact RC columns with stirrup spacing over rebar diameter  $s/d_b=12$  results in more than 50% increase of axial strength and 100% increase of maximum strains, as compared to similar RC columns with stirrup spacing  $s/d_b=8$  which corresponds to modern tie spacing requirements.
- Reinforced concrete columns with moderately buckled longitudinal bars, amounting to maximum deflection of rebars from verticality up to 15 mm for the 1/3-scaled specimens, can be effectively repaired by substituting the crushed concrete by fiber-reinforced repair mortar and continuous CFRP jacket without intervening in the buckled bars.
- A damage scale with increasing severity from I to V is introduced, according to which the damage of the specimens was assessed. Volumetric ratios of CFRP ranging from 0.3 to 1% for damage levels from I to V proved to be effective in preventing further buckling of the repaired specimens. It was observed that increased pre-existing damage level prior to retrofit affects adversely the mechanical properties of the retrofitted specimens.
- The axial stiffness of the retrofitted columns after the activation of the CFRP jacket is not apparently affected by the extent of prior damage. However, the initial stiffness before the activation of the CFRP jacket was shown to decrease as per 60% to 25% for damage levels from I to V, compared to similar columns with no

previous damage.

- The axial compressive strength of the retrofitted columns may be determined from design models which are intended for intact specimens by applying apposite reduction factors. In this study, the axial strength of the retrofitted columns was observed to drop by 90% to 65% for damage levels from I to V, in respect to intact columns, according to a proposed design model.
- The contribution of longitudinal reinforcement to the axial strength of a FRP-jacketed column reduces considerably when buckling of the rebars occurs. For this reason it is recommended that the longitudinal reinforcement should not be taken into account at the estimation of axial strength of FRP-confined RC columns with sparsely spaced stirrups.
- The proposed rapid repair method proved to be effective in upgrading seismically deficient short RC columns, both intact and moderately damaged, and could considerably facilitate retrofit works if appositely incorporated in design codes for earthquake retrofitting. Testing of larger scale specimens is deemed necessary to validate the results.

## Acknowledgments

The tests were performed in the Laboratory of RC Technology and Structures at the University of Thessaly, Greece. The author would like to thank Mr. E. Miliokas and Mr. I. Papanizos who have undertaken the tests as part of their undergraduate thesis in the School of Engineering, University of Thessaly, Volos, Greece, under the supervision of the author who served as Assistant Professor. The contribution of Mr. A. Koutselinis and Mr. T. Papatheocharis in manufacturing the specimens and technical advice at testing, respectively, as well as Sika Hellas SA for supplying the composite materials, are also gratefully acknowledged.

## References

- Anagnostopoulos, S. and Moretti, M. (2008), "Post-earthquake emergency assessment of building damage, safety and usability -Part 1: Technical issues", *Soil Dyn. Earthq. Eng.*, **28**(3), 223-232. <https://doi.org/10.1016/j.soildyn.2006.05.007>.
- ATC-20 (1991), Procedures for Post-Earthquake Evaluation of Buildings safety, Applied Technology Council., Governor's Office of Emergency Services, State of California, USA.
- ATC-32 (1996), Improved Seismic Design Criteria for California Bridges: Provisional Recommendations, Applied Technology Council, Redwood City, CA, USA.
- Bai, Y.L., Dai, J.G. and Teng, J.G. (2017), "Buckling of steel reinforcing bars in FRP-confined RC columns: An experimental study", *Constr. Build. Mater.*, **140**, 403-415. <https://doi.org/10.1016/j.conbuildmat.2017.02.149>.
- Bedirhanoglu, I., Ilki, A. and Triantafyllou, C.T. (2022), "Seismic behavior of repaired and externally FRP-jacketed short columns built with extremely low-strength concrete", *J. Compos. Constr.*, **26**(1), 04021068. [https://doi.org/10.1061/\(ASCE\)CC.1943-5614.0001179](https://doi.org/10.1061/(ASCE)CC.1943-5614.0001179).
- Bournas, D.A. and Triantafyllou T.C. (2011), "Bar buckling in RC columns confined with composite materials", *J. Compos. Constr.*, **15**(3), 393-403. [https://doi.org/10.1061/\(ASCE\)CC.1943-5614.0000180](https://doi.org/10.1061/(ASCE)CC.1943-5614.0000180).
- Carrillo, J., Valencia-Mina, W. and Bojórquez, E. (2020), "Compressive performance of square and low-strength concrete columns retrofitted with externally-bonded CFRP", *Mater. Today Commun.*, **23**, 1-12. <https://doi.org/10.1016/j.mtcomm.2019.100874>.
- C.E.B. Bull. No. 162 (1983), Assessment of Concrete Structures and Design Procedure for Upgrading (Redesign), Comite Euro-National du Beton, Paris, France.
- Chen, G.F., Ai, J. and Stratford, T.J. (2010), "Effect of geometric discontinuities in FRP-wrapped columns", *ASCE J. Compos. Constr.*, **14**(2), 136-145. [https://doi.org/10.1061/\(ASCE\)CC.1943-5614.0000053](https://doi.org/10.1061/(ASCE)CC.1943-5614.0000053).
- Cheng, C.T., Yang, J.C., Yeh, Y.K. and Chen, S.E. (2003), "Seismic performance of repaired hollow-bridge piers", *Constr. Build. Mater.*, **17**(5), 339-351. <https://doi.org/10.1007/BF02480517>.
- Demers, M. and Neale, K.W. (1999), "Confinement of reinforced concrete columns with fibre-reinforced composite sheets - An experimental study", *Can. J. Civil Eng.*, **26**, 226-241. <https://doi.org/10.1139/198-067>.
- Ding, M., Chen, X., Zhang, X., Liu, Z. and Lu, J. (2018), "Study on seismic strengthening of railway bridge pier with CFRP and concrete jackets", *Earthq. Struct.*, **15**(3), 275-283. <https://doi.org/10.12989/eas.2018.15.3.275>.
- Dirikgil, T. (2021), "Experimental investigation of the effects of concrete strength and axial load ratio on the performances of CFRP-wrapped and externally collared RC short columns", *Eng. Struct.*, **230**, 111647. <https://doi.org/10.1016/j.engstruct.2020.111647>.
- Elci, H. (2020), "Seismic strengthening of improperly repaired reinforced concrete columns using CFRP confinement", *Struct.*, **28**, 266-275. <https://doi.org/10.1016/j.jstruc.2020.08.072>.
- Eurocode 2 (2004), Design of Concrete Structures Part 1-1: General Rules and Rules for Buildings, European Committee for Standardization, Brussels, Belgium.
- Eurocode 8 (2004), Design of Structures for Earthquake Resistance Part 1: General Rules, Seismic Actions and Rules for Buildings, European Committee for Standardization, Brussels, Belgium.
- Eurocode 8 (2005), Design of Structures for Earthquake Resistance Part 3: Assessment and Retrofitting of Buildings, European Committee for Standardization, Brussels, Belgium.
- Fardis, M.N. (2009), *Seismic Design, Assessment and Retrofitting of Concrete Buildings Based on EN-Eurocode 8*, Springer Dordrecht, Germany.
- Faustino, P. and Chastre, C. (2016), "Damage effect on concrete columns confined with carbon composites", *ACI Struct. J.*, **113**(5), 951-962. <https://doi.org/10.14359/51687916>.
- Giamundo, V., Lignola, P., Prota, A. and Manfredi G. (2014), "Analytical evaluation of FRP wrapping effectiveness in restraining reinforcement bar buckling", *J. Struct. Eng.*, **140**(7), [https://doi.org/10.1061/\(ASCE\)ST.1943-541X.0000985](https://doi.org/10.1061/(ASCE)ST.1943-541X.0000985).
- He, R., Grelle, S., Sneed, L.H. and Belarbi, A. (2013), "Rapid repair of a severely damaged RC column having fractured bars using externally bonded CFRP", *Compos. Struct.*, **101**, 225-242. <https://doi.org/10.1016/j.compstruct.2013.02.012>.
- Ilki, A., Tore, E., Demir, C. and Comert, M. (2018), "Seismic performance of a full-scale FRP retrofitted sub-standard RC building", *Recent Advances in Earthquake Engineering in Europe: 16th European Conference on Earthquake Engineering-Thessaloniki 2018*, Thessaloniki, June.
- JBDPA (1991) (revised in 2001), Guideline for Post-Earthquake Damage Evaluation and Rehabilitation, The Japan Building Disaster Prevention Association, Japan.
- Jin, L., Chen, H., Wang, Z. and Du, X. (2020), "Size effect on

- axial compressive failure of CFRP-wrapped square concrete columns: Tests and simulations”, *Compos. Struct.*, **254**, 112843. <https://doi.org/10.1016/j.compstruct.2020.112843>.
- Kalogeropoulos, G. and Tsonos, A.D.G. (2019), “Improvement of the cyclic response of RC columns with inadequate lap splices-experimental and analytical investigation”, *Earthq. Struct.* **16**(3), 279-293. <https://doi.org/10.12989/eas.2019.16.3.279>.
- Kalogeropoulos, G., Tsonos, A.D.G. Konstandinidis, D. and Tsetines, S. (2016), “Pre-earthquake and post-earthquake retrofitting of poorly detailed exterior RC beam-to-column joints”, *Eng. Struct.*, **109**, 1-15. <https://doi.org/10.1016/j.engstruct.2015.11.009>.
- Kalogeropoulos, G., Tsonos, A.D.G. Konstandinidis, D. and Iakovidis, P. (2019a), “Earthquake-resistant rehabilitation of existing RC structures using high-strength steel fiber-reinforced concrete jackets”, *Earthq. Struct.*, **17**(1), 115-129. <https://doi.org/10.12989/eas.2019.17.1.115>.
- Kalogeropoulos, G., Tsonos, A.D.G. and Konstandinidis, D. (2019b), “Seismic behavior of RC columns with welded rebars or mechanical splices of reinforcement”, *Earthq. Struct.*, **17**(3), 297-306. <https://doi.org/10.12989/eas.2019.17.3.297>.
- Kam, W.Y., Pampanin, S. and Elwood, K. (2011), “Seismic performance of reinforced concrete buildings in the 22 February Christchurch (Lyttleton) earthquake”, *Bull. N. Z. Soc. Earthq. Eng.*, **44**(4), 239-278. <https://doi.org/10.1016/j.job.2021.103916>.
- KAN.EPE. (2012), Code for Retrofitting RC Buildings, EPPO of Greece, Athens, Greece.
- Karayannis, C., Chalioris, C. and Sirkelis, G. (2008), “Local retrofit of exterior beam-column joints using thin RC jackets-An experimental study”, *Earthq. Eng. Struct. Dyn.*, **37**, 727-746. <https://doi.org/10.1002/eqe.783>.
- Karayannis, C. and Goliass, E. (2018), “Full scale tests of RC joints with minor to moderate seismic damage repaired using C-FRP sheets”, *Earthq. Struct.*, **15**(6), 617-627. <https://doi.org/10.12989/eas.2018.15.6.617>.
- Kargaran, A. and Kheyroddin, A. (2020), “Experimental and numerical investigation of seismic retrofitting of RC square short columns using FRP composites”, *Eur. J. Env. Civil. Eng.*, **26**(10), 4619-4642. <https://doi.org/10.1080/19648189.2020.1858171>.
- Khan, A.R., Fareed, S. and Zahid, B. (2022), “Use of high strength technical textiles in strengthening of reinforced concrete structural elements”, *J. Text. Inst.*, **5**(5), 539-561. <https://doi.org/10.1080/00405000.2020.1870784>.
- Kono, S., Bechtoula, H., Sakashita, M., Tanaka, H., Watanabe, F. and Eberhard, M.O. (2006), “Damage assessment of reinforced concrete columns under high axial loading”, *ACI Special Publication*, **237**, 165-176.
- Lam, L. and Teng, J.G. (2004), “Ultimate condition of fiber reinforced polymer-confined concrete”, *J. Compos. Constr.*, **8**(6), 539-548. [https://doi.org/10.1061/\(ASCE\)1090-0268\(2004\)8:6\(539\)](https://doi.org/10.1061/(ASCE)1090-0268(2004)8:6(539)).
- Lim, J.C. and Ozbakkaloglu, T. (2015), “Hoop strains in FRP-confined concrete columns: Experimental observations”, *Mater. Struct.*, **48**, 2839-2854. <https://doi.org/10.1617/s11527-014-0358-8>.
- Maeda, M., Matsukawa, K. and Ito, Y. (2014), “Revision of guideline for post-earthquake damage evaluation of RC buildings in Japan”, *Tenth U.S. National Conference on Earthquake Engineering Frontiers of Earthquake Engineering*, Anchorage, Alaska, July.
- Mesbah, H.A. and Benzaid, R. (2017), “Damage-based stress-strain model of RC cylinders wrapped with CFRP composites”, *Adv. Concrete. Constr.*, **5**(5), 539-561. <https://doi.org/10.12989/acc.2017.5.5.539>.
- Moretti, M.L. (2008), “Concepts underlying reinforced concrete design: Time for reappraisal, by Michael D. Kotsovos/Author’s closure”, *ACI Struct. J.*, **105**(5), 645-646.
- Moretti, M.L. (2019), “Effectiveness of different confining configurations of FRP jackets for concrete columns”, *Struct. Eng. Mech.*, **72**(2), 155-168. <https://doi.org/10.12989/sem.2019.72.2.155>.
- Moretti, M. and Tassios, T.P. (2006), “Behavior and ductility of reinforced concrete short columns using global truss model”, *ACI Struct. J.*, **103**(3), 319-327.
- Moretti, M.L. and Tassios, T.P. (2007), “Behaviour of short columns subjected to cyclic shear displacements: Experimental results”, *Eng. Struct.*, **29**(8), 2018-2029. <http://doi.org/10.1016/j.engstruct.2006.11.001>.
- Moretti, M.L. and Tassios, T.P. (2013), “Design in shear of reinforced concrete columns”, *Earthq. Struct.*, **4**(3), 265-283. <http://doi.org/10.12989/eas.2013.4.3.265>.
- Moretti, M.L. and Arvanitopoulos, E. (2018), “Overlap length for confinement of carbon and glass FRP-jacketed concrete columns”, *Compos. Struct.*, **195**, 14-25. <https://doi.org/10.1016/j.compstruct.2018.04.038>.
- Moretti, M.L., Miliokas, E. and Papanizos, I. (2021a), “Retrofit of damaged RC columns using CFRP jackets”, *10th International Conference on FRP Composites in Civil Engineering*, İstanbul, December.
- Moretti, M.L., Miliokas, E. and Papanizos, I. (2021b), “Axial strength estimation of reinforced concrete columns confined through fiber reinforced polymer (FRP) jackets”, *J. Multidisc. Eng. Sci. Technol.*, **8**(4), 13804-13818.
- Ozcan, O., Binici, B. and Ozecebe, G. (2008), “Improving seismic performance of deficient reinforced concrete columns using carbon fiber-reinforced polymers”, *Eng. Struct.*, **30**, 1632-1646. <https://doi.org/10.1016/j.engstruct.2007.10.013>.
- Pampanin, S., Bolognini, D. and Pavese, A. (2007), “Performance-based seismic retrofit strategy for existing reinforced concrete frame systems using fiber-reinforced polymer composites”, *J. Compos. Constr.*, **11**(2), 211-226. [https://doi.org/10.1061/\(ASCE\)1090-0268\(2007\)11:2\(211\)](https://doi.org/10.1061/(ASCE)1090-0268(2007)11:2(211)).
- Pantazopoulou, S.J., Tastani, S.P., Thermou, G.E., Triantafyllou, T., Monti, G. and Bournas, D. (2016), “Background to the European seismic design provisions for retrofitting RC elements using FRP materials”, *Struct. Concrete*, **17**(2), 194-219. <https://doi.org/10.1002/suco.201500102>.
- Ricci, P., De Luca, F. and Verderame, G.M. (2011), “6th April 2009 L’Aquila earthquake, Italy: Reinforced concrete building performance”, *Bull. Earthq. Eng.*, **9**(1), 285-305. <https://doi.org/10.1007/s10518-010-9204-8>.
- Rousakis, T.C. and Karabinis, A.I. (2008), “Substandard reinforced concrete members subjected to compression: FRP confining effects”, *Mater. Struct. J.*, **41**, 1595-1611. <https://doi.org/10.1617/s11527-008-9351-4>.
- Rousakis, T.C. and Karabinis, A.I. (2012), “Adequately FRP confined reinforced concrete members under axial compressive monotonic loading”, *Mater. Struct. J.*, **45**, 957-75. <https://doi.org/10.1617/s11527-011-9810-1>.
- Saadatmanesh, H., Ehsani, M. and Jin, L. (1997), “Repair of earthquake-damaged RC columns with FRP wraps”, *ACI Struct. J.*, **94**(2), 206-215.
- Saiidi, M.S. and Cheng, Z. (2004), “Effectiveness of composites in earthquake damage repair of reinforced concrete flared columns”, *J. Compos. Constr.*, **8**(4), 306-314. [https://doi.org/10.1061/\(ASCE\)1090-0268\(2004\)8:4\(306\)](https://doi.org/10.1061/(ASCE)1090-0268(2004)8:4(306)).
- Sami, A., Khan, Q.Z., Azam, A., Raza, A. and Berradia, M. (2022), “Performance of repaired macro-synthetic structural fibers and glass-FRP-reinforced concrete columns”, *Iran. J. Sci. Technol. Trans. Civil Eng.*, **2022**, 1-12. <https://doi.org/10.1007/s40996-022-00966-y>.
- Tastani, S.P., Pantazopoulou, S.J., Zdomba, D., Plakantaras, V.

- and Akritidis, E. (2006), "Limitations of FRP jacketing in confining old-type reinforced concrete members in axial compression", *J. Compos. Constr.*, **10**(1), 13-25. [https://doi.org/10.1061/\(ASCE\)1090-0268\(2006\)10:1\(13\)](https://doi.org/10.1061/(ASCE)1090-0268(2006)10:1(13)).
- Tena-Colugna, A., Godínez-Domínguez, E.A. and Hernández-Ramírez, H. (2022), "Seismic retrofit and strengthening of buildings. Observations from the 2017 Puebla-Morelos earthquake in Mexico City", *J. Build. Eng.*, **47**, 103916. <https://doi.org/10.1016/j.jobbe.2021.103916>.
- Tsonos, A.D.G. (2008), "Effectiveness of CFRP-jackets and r/c-jackets in post-earthquake and pre-earthquake retrofitting of beam-column subassemblages", *Eng. Struct.*, **30**(3), 777-793. <https://doi.org/10.1016/j.engstruct.2007.05.008>.
- Vicente, R.S., Rodrigues, H., Varum, H., Costa, A. and da Silva, J.A.R.M. (2012), "Performance of masonry enclosure walls: Lessons learned from recent earthquakes", *Earthq. Eng. Eng. Vib.*, **11**(4), 23-34. <https://doi.org/10.1007/s11803-012-0095-3>.
- Vosooghi, A. and Saiidi, S. (2012), "Design guidelines for rapid repair of earthquake-damaged circular RC bridge columns using CFRP", *J. Bridge Eng.*, **91**(4), 1301-1328. [https://doi.org/10.1061/\(ASCE\)BE.1943-5592.0000426](https://doi.org/10.1061/(ASCE)BE.1943-5592.0000426).
- Vosooghi, A. and Saiidi, M. (2013), "Shake-table studies of repaired reinforced concrete bridge columns using carbon fiber-reinforced polymer fabrics", *ACI Struct. J.*, **110**(1), 105-114.
- Wang, H., Sun, B. and Chen, H. (2022), "Performance-based seismic evaluation and practical retrofit techniques for buildings in China", *Earthq. Struct.*, **22**(5), 487-502. <https://doi.org/10.12989/eas.2022.22.5.487>.
- Wang, Z., Wang, D., Smith, S.T. and Lu, D. (2012), "CFRP-confined square RC columns I: Experimental investigation", *J. Compos. Constr.*, **16**(2), 150-160. [https://doi.org/10.1061/\(ASCE\)CC.1943-5614.0000245](https://doi.org/10.1061/(ASCE)CC.1943-5614.0000245).
- Yamada, M. and Furui, S. (1968), "Shear resistance and explosive cleavage failure of reinforced concrete members subjected to axial load", *8<sup>th</sup> the International Association for Bridge and Structural Engineering (IABSE)*, New York, September.
- Zhiguo, S., Hongnan, L., Kaiming, B., Bingjun, S. and Dongsheng, W. (2017), "Rapid repair techniques for severely earthquake-damaged circular bridge piers with flexural failure mode", *Earthq. Eng. Eng. Vib.*, **16**(2), 415-433. <https://doi.org/10.1007/s11803-017-0390-0>.